Mining EEG scalp maps of independent components related to HCT tasks

A. R. Teixeira[1], I.M. Santos[3], E.W. Lang [4] and A.M. Tomé[2]

***Abstract*— This work presents an unsupervised mining strategy, applied to an independent component analysis (ICA) of segments of data collected while participants are answering to the items of the Halstead Category Test (HCT). This new methodology was developed to achieve signal components at trial level and therefore to study signal dynamics which are not available within participants' ensemble average signals. The study will be focused on the signal component that can be elicited by the binary visual feedback which is part of the HCT protocol. The experimental study is conducted using a cohort of 58 participants.**

I. INTRODUCTION

The Halstead Category Test is a popular measure of abstraction, concept formation, and logical analysis skills. The test is applied since long clinically, and, to facilitate its administration, computer versions of the test are now available [1]. Traditionally, the test provides only an overall error score indicative of global impairment, but there is a recent interest to develop and validate several scoring subscales to reflect the changes of the participant's performance across a sequence of items of the test [2]. The item's stimuli consist of geometric figures or designs, and the participant was asked to indicate a number between 1 and 4, which each stimulus suggests. After every response, visual feedback on whether the response was correct or incorrect is provided. The feedback helps participants to adjust their strategy to answer to the next item. In this work, a computer version of the test was used and the EEG was recorded while the participants answered to the items of the test. The main aim of the study was to analyse signals while the participants performed the test. The hypothesis was that if an error was indicated by means of an explicit feedback, a feedback-related negativity (FRN) signal could be reliably measured at the fronto-central region at 200 - 300 ms after the feedback. In [3] it was possible to find this signal signature in denoised, ensemble-averaged signals calculated for correct and incorrect responses. In the study, it was necessary to denoise the signals, because trial removal would discard most of the recording. It has to be noticed that with the described acquisition scenario it was useless to instruct participants to avoid movements or blinks, and therefore common strategies to eliminate or correct segments with artifacts were not applicable.

[1] ESEC Instituto Politécnico Coimbra 3030- 329 Coimbra, Portugal ateixeira@ua.pt

[2] DETI/ IEETA University of Aveiro, 3810-193 Aveiro,Portugal ana@ua.pt

[3] CINTESIS, Departamento de Educação e Psicologia, Universidade Aveiro 3810-193 Aveiro, Portugal isabel.santos@ua.pt

[4] Institute of Biophysics,CIML Group, University of Regensburg, 93040 Regensburg, Germany elmar.lang@ur.de

Electroencephalogram signals have been used in applications where the signals were registered in conditions less constrained than in traditional brain cognitive studies. These new applications introduced signal processing and machine learning techniques in order to extract useful information from the signals. Exploratory matrix factorizations techniques, like ICA, are widely used to decompose multichannel recordings and to remove components related with noise sources, like blinks and other biological interferences [4]. The selection of components is one of the most studied problems when ICA is used to decompose signals [5], [6]. Another strategy, introduced in Brain Computer Interfaces, is the so-called common spatial filtering [7], whose goal is to estimate the component that enhances the difference between the tasks performed while the EEG is recorded. In that case the computation of the model is supervised, as the label information is relevant to estimate that particular column of the de-mixing matrix [8]. In this work, we exploit unsupervised techniques to identify components which correspond to clusters of scalp maps. This methodology was applied to find the component that could be related with the FRN component at single trial level. The single-trial component of all participants are averaged in the four sub-tests of the HCT test. It will be shown that the trial level signals can also be studied.

The paper is organized as follows: the section Methods and Materials presents the organization of the HCT test, the methodology to find template scalp methods and the signal signatures. Finally Results and Conclusions are presented.

II. MATERIAL AND METHODS

The signal processing steps are performed at different levels: single-trial level, participant level and group level. The single-trial level comprises the application of a standard ICA [9],[10]. At participant level, the K-Means clustering algorithm [11] is applied to features extracted from the normalized columns of the mixing matrices. The templates of the clusters are used to guide the selection of signal components with specific scalp localizations. These signals can be compared at group level as average ERP components as well as be analysed at sub-test level or single-trial level.

A. Participants and HCT test

Fifty eight participants (39 females and 19 males) were enrolled in the study. The EEG was continuously registered and electrodes were placed according to the $10-20$ system with an Easy - Cap comprising $C = 26$ channels and were recorded, using a sampling rate of $1\ kHz$. The HCT involves

978-1-5386-1311-5/19/$31.00 ©2019 IEEE

the presentation of 208 trials divided into seven subtests [1]. This test is used to measure a person's ability to formulate abstract principles based on the feedback received after their response to each specific test question. The visual feedback provided indicates if the participant's response was right or wrong. Note that at trial level, the signal segment comprises the following sequence of time stamps: presentation of the stimulus, the participant's response and the feedback information. The time interval between stimulus presentation and the participant's response is variable, while the time between response and feedback is $1500\ ms$. The average time for the participant to answer was $1790\ ms \pm 400\ ms$.

B. Scalp Templates

The processing chain is based on the application of a standard ICA algorithm to the segment of data comprising visual stimulus, the response and the feedback. Therefore, the multichannel segment with $9\ s$, $6\ s$ before and $3\ s$ after the response is chosen to perform the ICA decomposition. After this step, the multichannel trial segment $\mathbf{X}^{(t)}$ is modelled as

$$\mathbf{X}^{(t)} = \mathbf{A}^{(t)}\mathbf{S}^{(t)} \tag{1}$$

where $\mathbf{A}^{(t)}$ is the inverse (or pseudo-inverse) of the de-mixing matrix, and $\mathbf{S}^{(t)}$ is the matrix with the corresponding sources estimated by the algorithm. In order to have an identical scale in all trials, the elements of the matrix $\mathbf{A}^{(t)}$ are normalized to the range $[0 \quad 1]$. To achieve this goal, all absolute values of the elements of the matrix are divided by the $L2$ norm of the corresponding row. Afterwards, the entries of each column are pooled according to the their scalp localization (pre-frontal, frontal, fronto-central, occipital, parietal and temporal). The median value of each scalp region then forms the feature vector [12]. These feature vectors of all trials are then clustered and the templates are estimated as it is described on the block diagram of figure 1. The centroids of the clusters in the original dimension $C = 26$ are then calculated . In order to compare participants, the centroids are re-ordered so that the first cluster has the largest activation values on the frontal region, the second cluster the largest activations in fronto-central and so on (see the example of figure 1).

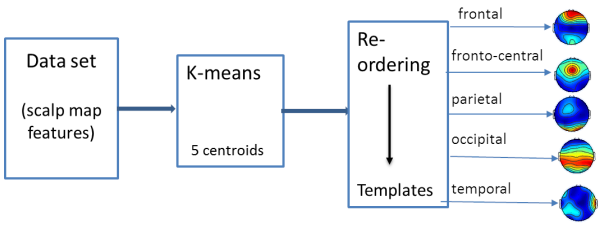

Fig. 1. Estimating the centroids of the clusters: on the right scalp map templates belonging to one of the participants.

After clustering the elements, e.g. the columns of the normalized mixing matrices, of each cluster are also known. Note that at trial level the $C = 26$ columns of the normalized matrix are then assigned to the 5 clusters.

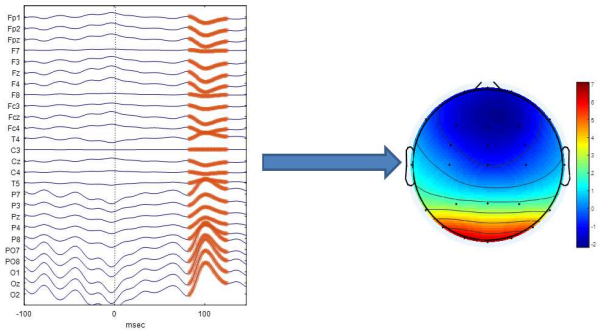

Fig. 2. Reconstruction: The selected component back-projected to the scalp sensors. The topoplot is estimated mean amplitudes in an interval of $5\,ms$ of the peak detected between $[80 \quad 100]$ms in channel $O1$. The visual component $P100$ is clearly visible on the occipital sensors.

C. Cluster signatures

At trial level, a particular cluster signature is chosen using a template matching strategy. Within trial elements of a cluster, the element closest to the template is chosen. The cosine distance is used as similarity measure to compare the normalized scalp maps with the centroid. Therefore, assuming that the selected scalp map has an index i, and using the outer product model to represent the product of two matrices, eqn. 1 is a sum of C matrices. In particular, the contribution of the i-th scalp map and the corresponding component is written as

$$\hat{\mathbf{X}}^{(t)} = \mathbf{A}^{(t)}_{*i}\mathbf{S}^{(t)}_{i*}$$

where $\mathbf{A}_{*i}$ represents the i-th column of the mixing matrix and $\mathbf{S}_{i*}$ represents i-th row of the source matrix. The figure 2 illustrates the result of this procedure, showing a short segment of the multichannel signals, which corresponds to the occipital template. The segment includes the stimulus presentation (t=0), and the signals show a clear positive peak around $100\ ms$. The peak is naturally more visible in the occipital regions as it is shown in the topoplot of the on the right side of the figure.

III. Results

Most reward-related electroencephalogram (EEG) studies focus on the feedback-related negativity (FRN). This component is usually measured approximately $200 - 300\ ms$ post-feedback at a single electrode in the fronto-central area (Cz, Fz or FCz). The procedure described in the methodology section is applied to identify this component in the reconstructed version of the component related with fronto-central cluster of each trial. Each trial on the signals corresponds to the presentation of one of the visual items of the HCT test.

A. HCT and Participant's performance

The HCT is divided into seven subtests. The participants are instructed to determine or guess the correct number, ranging from one to four, based on their conceptualization of the abstract principle represented by the stimulus. The participant receives visual feedback after each response, to

TABLE I

PARTICIPANT'S RESPONSES ON THE FIRST AND LAST THREE TRIALS: ENTRIES REPRESENT THE NUMBER OF PARTICIPANTS ANSWERING 0, 1, 2 OR 3 TIMES *wrong*.

	First three trials				Last three trials			
# *wrong*	0	1	2	3	0	1	2	3
Subtest III	7	7	30	14	42	10	6	0
Subtest IV	31	19	5	3	40	9	6	3
Subtest V	9	19	16	14	47	9	2	0
Subtest VI	42	9	5	2	20	13	22	3

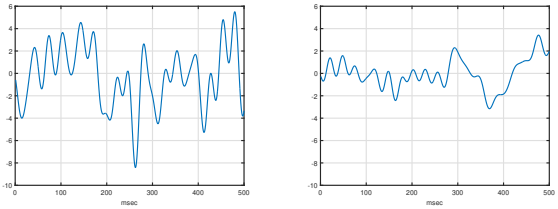

Fig. 3. Subtest III: recontructed component at FCz scalp position of one participant.*Left*: three first trials;*Right*: three last trials.

indicate if his response was right or wrong. Furthermore, the participant knows when a sub-test starts, and at the beginning of the test he/she is informed that the underlying abstract principle may(or may not) change from one sub-test to the next. The participant is never sure of this on the first trials, and he will only be able to determine the correct abstract principle on the basis of the feedback he receives about his performance. Each of the sub-sets III, IV , V and VI comprise 40 trials. The subtests III and IV assess spatial/positional reasoning and subtests V and VI assess proportional reasoning. In general, the participants provide more often wrong answers in subtest III and subtest V than in subtests IV and VI. Anyway, note that the number of wrong answers in a total of 40 trials is usually not more than 15. The table I shows how the participants perform in the first three trials and in the last three trials of each subtest. On the first three trials, the number of participants giving wrong responses is larger on substests III and V. On the other hand, more than half of participants do not give any wrong response on the beginning of the subtests IV and V. Note that the last case represents two subtests where the underlying principle did not change from the previous subtest. On the last three trials of each subtest, more than half of the participants do not have any wrong answer in three of the subtests.

In this case, we were interested in studying the FRN. In particular, we were interested in subtest transitions, when participants are still unsure about the abstract principle underlying the following subtest.

B. Participant level analysis

For each participant the transitions between the subtests were analysed. With that purpose, the first three trials and the last three trials were averaged. The figures 3 and 4 illustrate the component reconstructed at FCz scalp position. In both subtests, the signals show that the most negative peak occurs

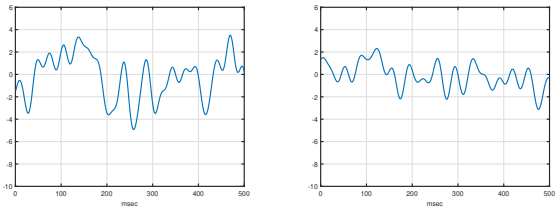

Fig. 4. Subtest IV: recontructed component at FCz scalp position of one partipant *Left*: three first trials;*Right*: three last trials.

in the time window of the FRN event on the first trials. However in subtest III the negativity is larger than in subset IV.

For the last three trials of the subtests, the FRN related pattern is not clearly defined. The signals show negative peaks with smaller amplitude in other time intervals and in the FRN window more than one negative peak is presented. The visual inspection illustrated here was performed to the subtests V an VI and the results were similar.

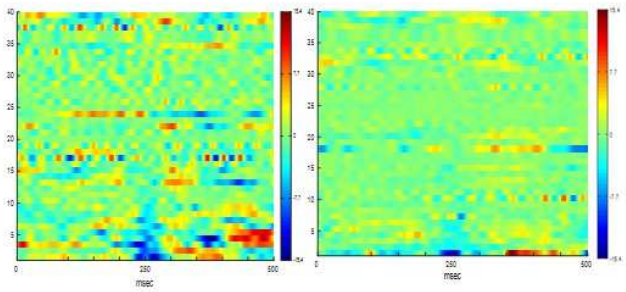

Fig. 5. ERP average image of the back-projected component, at scalp location FCz, related to the fronto-central.*Left*: Subtest III;*Right*: Subtest IV.

C. Inter-participant subtest analysis

The fronto-central time signatures are calculated for all trials. Note that the subtests of the HCT test have the same number of trials and the participants answer while performing the same task. Therefore, after reconstructing the fronto-central signature, the signals are now averaged for every participant. For each scalp position, it is possible to represent the information as an image following the strategy suggested in the EEGLAB platform [13]. Then the i-th row of the image represents the average of i-th trial across all participants. The figures 5 and 6 illustrate the results for the 40 trials of the four subsets.

Both spatial or proportional reasoning sub-tests have a similar outcome. The transition subtests (III and V) present on the first trials a clear negativity, with latency around 250 ms, as can be seen on the left images of both figures. The images on the right side, related with subtests where the underlying principle does not change, the negativity, at that latency, is present but less intense. Note as well that in all cases this negativy is visible sequentially on the 10 to 15 trials but at later trials is less negative.

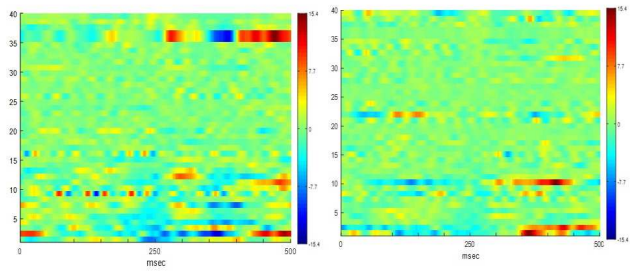

Fig. 6. ERP average image of the back-projected component, at scalp location FCz, related to the fronto-central cluster. *Left*: Subtest V; *Right*: Subtest VI.

The topoplots represent the component reconstructed in all scalp positions (see fig 7). The topoplots consistently show a negativity in the fronto-central region for the three trials of the test. Note that for convenience of representation, the topoplots have different scales. On the beginning of the test, the amplitude range, between $[-15 \quad 4]\mu V$, is smaller and more localized. For the 10-th trial, the amplitude is less negative with a range of $[-6 \quad 1]\mu V$ and spreads into the frontal region. The 38-th- trial shows a similar pattern within an amplitude range of $[-3 \quad 1]\mu V$.

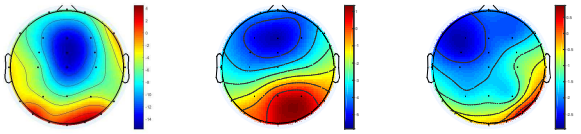

Fig. 7. Topoplots of the reconstructed component averaged for all participants. The i-th trial: *Left*: $i = 1$; *Middle*:$i = 10$; *Right*:$i = 38$. The mean amplitude in an interval of 20ms around the latency of the negative peak, detected at FCz, occuring between $[200 \quad 300]ms$.

IV. Conclusions

In this work an unsupervised methodology is proposed which combines an ICA decomposition with a K-means clustering to identify signal signatures related with the binary (failure and success) feedback of the HCT. Different studies have been conducted following the methodology explained in [12]. This work presents the results of the application of this methodology to characterize specific phases of the HCT test. The main conclusion supports that an FRN signal is present whenever the participant is uncertain about the outcome. For instance, between the transition of subtests, where the principle does not change, the number of wrong answers decrease, still the FRN is present. Future work shall comprise the study of other characteristics of the signals as is nowadays suggested in brain cognitive studies [14].

ACKNOWLEDGMENT

This work was partially supported by national funds through FCT—Foundation for Science and Technology, within the RD Units IEETA (UID/CEC/00127/ 2013) and CINTESIS (UID/IC/4255/2013), and by European funds through FEDER, under the COMPETE 2020 and Portugal 2020 programs, in the context of the projects PTDC/EEI-SII/6608/2014 and POCI-01-0145-FEDER-007746. This research was also supported by Bial Foundation with the Grant ref. 136/08 to Isabel M Santos.

References

[1] G. M. Silk-Eglit, J. H. Gunner, A. S. Miele, J. K. Lynch, and R. J. McCaffrey, "A comparison of the standard category test with a new computer version," *Applied Neuropsychology: Adult*, vol. 21, no. 1, pp. 9–13, 2014.

[2] S. Roye, M. Calamia, K. Greve, K. Bianchini, L. Aguerrevere, and K. Curtis, "Further validation of booklet category test subscales for learning, set loss, and memory in a mixed clinical sample," *Applied Neuropsychology: Adult*, vol. 25, no. 1, pp. 11–18, 2018.

[3] I. Santos, A. Teixeira, A. Tomé, A. Pereira, P. Rodrigues, P. Vagos, J. Costa, M. Carrito, B. Oliveira, N. DeFilippis, and C. Silva, "ERP correlates of error processing during performance on the Halstead Category Test," *International Journal of Psychophysiology*, vol. 106, pp. 97–105, 2016.

[4] I. Daly, N. Nicolaou, S. J. Nasuto, and K. Warwick, "Automated artifact removal from the electroencephalogram: a comparative study." *Clinical EEG and neuroscience*, vol. 44, no. 4, pp. 291–306, Oct 2013.

[5] M. Chaumon, D. V. Bishop, and N. A. Busch, "A practical guide to the selection of independent components of the electroencephalogram for artifact correction," *Journal of Neuroscience Methods*, vol. 250, pp. 47–63, Jul 2015.

[6] T. Radüntz, J. Scouten, O. Hochmuth, and B. Meffert, "Automated EEG artifact elimination by applying machine learning algorithms to ICA-based features," *Journal of Neural Engineering*, vol. 14, no. 4, p. 046004, 2017.

[7] B. Blankertz, R. Tomioka, S. Lemm, M. Kawanabe, and K. r. Muller, "Optimizing Spatial filters for Robust EEG Single-Trial Analysis," *IEEE Signal Processing Magazine*, vol. 25, no. 1, pp. 41–56, 2008.

[8] Y. Wang and T. P. Jung, *Improving brain- computer interfaces using independent component analysis*. Springer Berlin Heidelberg, 2013, pp. 67–83.

[9] A. Belouchrani, K. Abed-Meraim, J. F. Cardoso, and E. Moulines, "A blind source separation technique using second-order statistics," *IEEE Transactions on Signal Processing*, vol. 45, no. 2, pp. 434–444, Feb 1997.

[10] P. Common and C. Jutten, *Handbook of Blind Source Separation: Independent Component Analysis and its Applications*. Academic Press, 2010.

[11] A. K. Jain, "Data clustering: 50 years beyond k-means," *Pattern Recognition Letters*, vol. 31, no. 8, pp. 651 – 666, 2010.

[12] A. R. Teixeira, I. M. Santos, and A. M. Tomé, "Identifying evoked potential response patterns using independent component analysis and unsupervised learning," *Biomedical Physics and Engineering Express*, vol. 5, no. 1, p. 015019, 2019. [Online]. Available: http://stacks.iop.org/2057-1976/5/i=1/a=015019

[13] A. Delorme and S. Makeig, "EEGLAB: an open source toolbox for analysis of single-trial EEG dynamics including independent component analysis," *Journal of Neuroscience Methods*, vol. 134, no. 1, pp. 9 – 2, 2004.

[14] J. E. Glazer, N. J. Kelley, N. Pornpattananangkul, V. A. Mittal, and R. Nusslock, "Beyond the FRN: Broadening the time-course of EEG and ERP components implicated in reward processing," *International Journal of Psychophysiology*, vol. 132, pp. 184 – 202, 2018, reward and Feedback Processing: State of the Field, Best Practices and Future Directions.